Physical Review & Research International
4(1): 40-50, 2014

SCIENCEDOMAIN ***international***
www.sciencedomain.org

Microhardness Anisotropy and the Indentation Size Effect in Single Crystal Magnesium Fluoride, MgF_2

Lei Zhang[1*] and Richard C. Bradt[2]

[1]*Chemistry Department, Winston Salem State University, Winston Salem, NC 27110, USA.*
[2]*Department of Metallurgical and Materials Engineering, the University of Alabama, Tuscaloosa, AL 35487-0202, USA.*

Authors' contributions

This work was carried out in collaboration between both authors. Author RCB designed the study, wrote the protocol, and wrote the first draft of the manuscript. Author LZ performed the statistical analysis, managed the analyses of the study, and managed the literature searches. Both authors read and approved the final manuscript.

Research Article

Received 23rd July 2013
Accepted 14th September 2013
Published 7th October 2013

ABSTRACT

The Knoop microhardness anisotropy profile was determined on the (001) of MgF_2 which has microhardness maxima in the <110> and minima in the <100>. This anisotropy is the same as TiO_2 and SnO_2 which also have the rutile crystal structure. This indicates that the slip systems are the same for MgF_2 as the other two rutile structures. The (001) microhardness of MgF_2 is the most anisotropic of these three rutile structures. The three rutile structures are compared with regard to their absolute hardness values. MgF_2 is much softer than the oxides, only about half the hardness of SnO_2 and a third that of TiO_2. It reflects the bond strengths as related to the single crystal elastic constants. The hardness of MgF_2 is similar to, but slightly harder than the cubic alkaline earth fluorides, all of which have the fluorite structure. The indentation size effect of MgF_2 on the (001) for the Knoop indenter over the range of test loads from 10g to 300g was determined. The ISE of MgF_2 is less pronounced than those of TiO_2 and SnO_2.

Keywords: Microhardness; anisotropy; indentation size effect; MgF_2.

[*]*Corresponding author: Email: zhangl@wssu.edu;*

1. INTRODUCTION

MgF_2 is an alkaline earth fluoride with the tetragonal rutile crystal structure. The alkaline earth fluorides CaF_2, SrF_2 and BaF_2 all crystallize in the cubic fluorite structure [1]. MgF_2 crystallizes in the rutile structure because of the small Mg^{2+}cation. The mineral name of MgF_2 is sellaite. It is not abundant in nature and must be produced synthetically. It is birefringent and of commercial interest for its optical properties in the UV and IR ranges. MgF_2 is transparent over the wide range of wavelengths from ~0.12µm to ~7.50µm. It is durable and does not easily produce color centers when irradiated. This latter feature makes it desirable for laser windows, polarizers and for optical lenses. It is sometimes used for the antireflective coatings on the lenses of glass spectacles and cameras because of its index of refraction. Although MgF_2 has outstanding optical properties, there is a paucity of information on its mechanical properties, especially in comparison with other alkaline earth fluorides and rutile crystal structures.

One of the simplest mechanical property measurements of a material is the microhardness [2]. In addition to just the magnitude of the microhardness, there are two other important aspects to the microhardness of single crystals. One is the hardness anisotropy profile which describes the directional dependence of the microhardness on a specific crystal plane. It is determined by the slip systems of the structure. The other important hardness feature is the indentation size effect, or ISE of the material. The ISE is the increase of the measured microhardness with a decrease in the indentation test load, or the indentation size. Smaller indentations produce higher hardness values which can increase substantially in the low load indentation microhardness regime. The ISE is critically important with regard to nanohardness measurements [3,4].

These two characteristics, the hardness anisotropy profile and the ISE, are much more descriptive of the hardness of a material than just the Moh's scratch hardness, which has been reported to be ~6 for MgF_2, or any single hardness value, which has been reported for MgF_2 to be ~415 kg/mm^2. The cubic fluorides are slightly softer than MgF_2, only ~4 on the Mohs scale. This paper reports Knoop microhardness measurements of those two important aspects of the hardness on the (001) plane of tetragonal MgF_2. The [001] is the common crystal growth direction for synthetic MgF_2 single crystals. The microhardness, its anisotropy on the {001} and the ISE of MgF_2 for the {001} <100> indentations are then compared with similar results for single crystals of rutile (TiO_2) and cassiterite (SnO_2) for the same orientations and ranges of indentation test loads [5-7]. The purpose of this paper is to profile microhardness anisotropy and to study the indentation size effect of single crystal - MgF_2.

2. MATERIALS AND METHODS

The single crystal MgF_2 measured in this study was commercially grown in the <001> by Corning Tropel[8]. The ~7.5 cm diameter crystal with 13 mm thickness was transparent. A (001) plane specimen was prepared for hardness testing by diamond slicing from the crystal and then polishing with successively finer abrasives and finally with ¼ µm diamond paste in a vibratory polisher. The indentation testing surface, the (001), appeared to be smooth and scratch-free when viewed optically at 100x. The polished test specimen was neither annealed, nor etched before the Knoop microhardness measurements were taken.

Knoop microhardnesses were chosen for the hardness characterization because the long shallow indentations which are produced by a Knoop indenter are not as prone to

indentation cracking as are sharper indenters, an event which casts doubt on the credibility of any hardness measurements. The several crystallographic directions on the (001) which are specified for the microhardnesses are parallel to the long axis of the pyramidal Knoop impression.

A 360ºgoniometer was affixed to a Buehler Micromet 2004 Microhardness Testing Machine [9] to hold the crystal in position and to orient the crystal with respect to the crystallographic directions on the (001) plane. For indentation testing, the crystal was mounted using silly-putty and a hand press to insure that the measurement surface was always perpendicular to the penetrating indenter during the testing. The pyramidal impression length measurements were made immediately after removal of the indenter. Microhardess values were then calculated from the length of the long impression axis, d, and the standard Knoop microhardness formula:

$$H_K = 14.230\ P / d^2\ (\mathrm{kgf/mm^2}), \qquad (1)$$

where P is the indentation test load [10]. For each of the reported hardness values at the different orientations, ten distinct, perfectly symmetrical indentations were measured and their values were averaged. No cracked indentations were observed for the MgF_2 crystal as MgF_2 is relatively soft and produces well defined Knoop indentations.

The Knoop microhardness values for the rutile, TiO_2 and the cassiterite, SnO_2 for comparison with the MgF_2 measurements of this study were from previously published microhardness results for TiO_2 and SnO_2 [5-7]. Because of the absolute microhardness differences between the oxides and the fluoride, for a direct comparison of the three, several of the results were extrapolated using the (P/d vs. d) straight line relationship, which has been demonstrated to describe Knoop microhardness data. This technique, and the use of a broken ordinate scale on the figures, enabled the graphical representation of all three crystals on the same figure, facilitating a direct comparison.

3. RESULTS AND DISCUSSION

3.1 Microhardness Anisotropy Profiles

Fig. 1 illustrates the Knoop microhardness profiles on the basal plane for the three rutile structure crystals at the 100g indentation test load. The ordinate scale is broken to accommodate the oxides and the MgF_2. Magnesium fluorideis much softer than the two oxides, but the microhardness profiles are similar for all three. Each has microhardness minima in the <100> and a maximum in the <110>. This hardness profile occurs because of the crystallography of the slip systems about diamond imprint to accommodate the indentation deformation by dislocation plastic flow. Hardness anisotropy profiles are dominated by the resolved shear stress on the primary slip system of the crystal structure. McColm [2] discusses this issue in relation to the resolved shear stresses on the primary slip system and its role in the determination of the hardness anisotropy profiles for different crystals. Li and Bradt [11] have tabulated the hardness profiles for numerous crystal structures. The microhardness anisotropy profiles in Fig. 1 indicate that all three of these rutile structure crystals have the same primary slip system. It is in agreement with the {110} <001> as reported independently by Hirthe et al. [12].

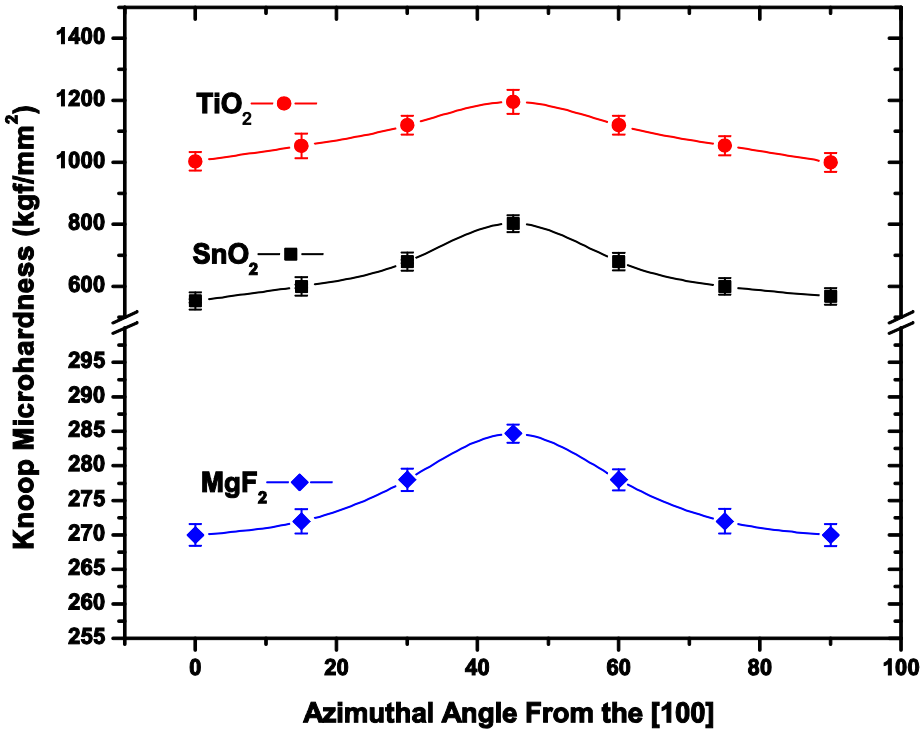

Fig. 1. The Knoop microhardness profiles on the (001) from the [100] to the [010]. A maximum occurs for the [110] and minima are at the [100] and the [010] for all three of these rutile structure crystals, TiO_2, SnO_2 and MgF_2.

Although, the microhardness profiles on the (001) are similar for all three crystals, the maxima and minima values are at different absolute levels for each crystal. There is no standard methodology to quantitatively describe the extent of this anisotropy and quantitatively compare the microhardness profiles of these crystals as none has been derived or advanced to quantify and describe the anisotropy. For purposes of comparison, a direct analogy to that which has been used to describe elastic anisotropy is applied. It is the description for the elastic anisotropy after Zener, as discussed by Chung and Buessem[13]. It is the hardness difference between the maximum and the minimum, (H_{max}– H_{min}), normalized by the square root of their product $\sqrt{H_{max} x H_{min}}$:

$$(H_{max} - H_{min}) \ / \ \sqrt{H_{max} x \ H_{min}}. \qquad (2)$$

Another related possibility for Equation (2) is to replace the square root term with one half of the sum of the maximum and minimum for the hardness normalization.

The Knoop microhardness anisotropy for each of the three rutile structures on the (001) calculated by Equation 2, are listed in Table 1 below:

Table 1. Calculated microhardness anisotropies on the crystal (001) planes

Crystal	H_{max}	H_{min}	Anisotropy
MgF_2	360	260	0.327
TiO_2	1186	1003	0.168
SnO_2	795	600	0.282

These values indicate that TiO_2 is the least anisotropic of these three structures and that the MgF_2 is the most anisotropic in its Knoop microhardness. Cassiterite is similar to MgF_2, also highly anisotropic in its microhardness profile on the (001) basal plane.

It is of interest to compare the magnitudes of the microhardnesses anisotropies with those of the elastic constants for these crystals [14]. The single crystal elastic constants of cassiterite, SnO_2, do not appear to have been measured and reported, but it is still of interest to compare the elastic anisotropies of the MgF_2 and the TiO_2 with those of the microhardnesses. The single crystal elastic stiffnesses constants are listed in Table 2.

Table 2. Single crystal elastic stiffnesses of MgF_2 and TiO_2 [14]

Crystal	C_{11}	C_{12}	C_{33}	C_{13}	C_{44}	C_{66}
MgF_2	1.40	0.89	2.05	0.63	0.57	0.96
TiO_2	27.14	17.8	48.39	14.96	12.44	19.48

As MgF_2 is a weakened form of the rutile crystal structure (2x1=2 versus 4x2=8 for TiO_2), it is not surprising that MgF_2 has much lower elastic stiffnesses than TiO_2. The values listed in Table 2 indicate that the approximate ionic charge ratio factor, a difference of four (2 vs. 8) for the two is not very descriptive, one would expect MgF2 to have a weaker columbic force given that the ionic species have a lesser charge. In fact the effects of some covalent bonding in the TiO_2 suggest much stronger bonds than might be expected on an ionic bonding. From the bond strengths as reflected by the elastic stiffnesses, it is not surprising that TiO_2 is much harder than the MgF_2. Since the microhardness of cassiterite is intermediate to that of MgF_2 and TiO_2, when the SnO_2 elastic stiffnesses are eventually measured and reported, they may be expected to be intermediate to those of MgF_2 and TiO_2, but nearer to those of the TiO_2.

Because of the complexity of the elastic anisotropy and the crystallography of the dislocation plastic flow processes beneath an indenter during indentation, a simple estimate will be made to compare the normal (C_{11} and C_{33}) and shear (C_{44} and C_{66}) anisotropies for MgF_2 and TiO_2. Applying a modified form of the previous equation that was applied for normalizing the microhardness, but adjusted for the elastic anisotropy:

$$C_{ii} - C_{jj} / \sqrt{C_{ii} x C_{jj}}, \quad (3)$$

yields separate normal (C_{11} and C_{33}) and shear (C_{44} and C_{66}) elastic anisotropies for the MgF_2 and the TiO_2. These two elastic anisotropies are 0.38 and 0.53 respectively for the MgF_2 and 0.59 and 0.46 for the TiO_2. In absolute magnitude, these are greater than, but are similar to the microhardness anisotropies. They do not reveal any systematic trend for these rutile structures. The crystals are similar in their elastic anisotropies in spite of the large differences in their elastic stiffnesses.

3.2 The Indentation Size Effect, the ISE

Fig. 2 presents the (001) [100] Knoopmicrohardness values for indentation test loads from 10g to 90g for the MgF_2, TiO_2 and SnO_2. The indentation size effect or ISE is evident for these three rutile crystals. All three crystals exhibit a distinct decrease of their microhardnesses with an increase of the indentation testing load, or conversely an increase of the microhardness with a decrease in the testing load. The TiO_2 and SnO_2 both have much higher hardnesses than the MgF_2, but all three of these crystals have hardness versus indentation test load plots that are quite similar and almost parallel in their ISE trends. Just as these three rutile structure crystals were observed to have similar microhardness profiles, they also have similar ISE trends. Although these microhardness values are for indentation on the (001) [100], similar results could be obtained for other crystal orientations. The scale of the ordinate is again broken to accommodate the results for all on the same figure.

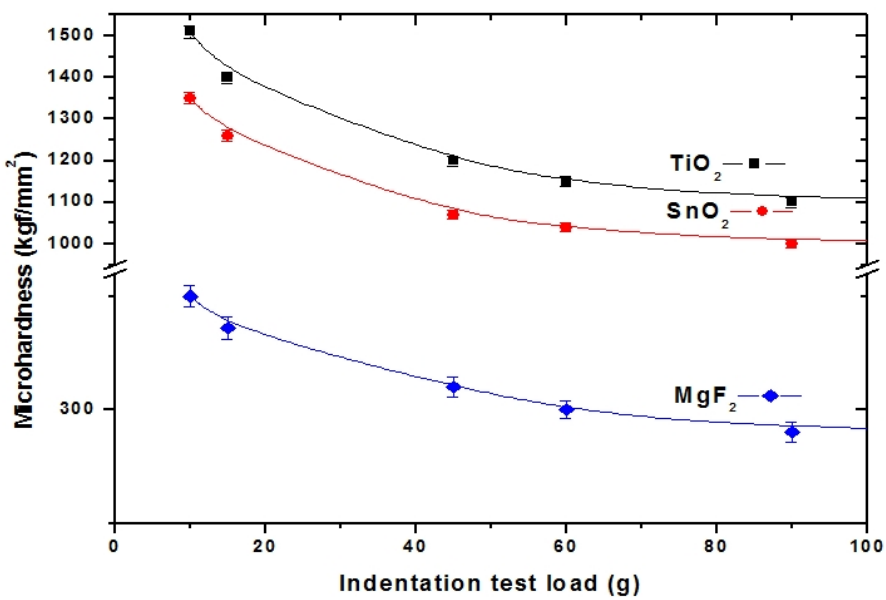

Fig. 2. The effect of indentation test load on the microhardness, the ISE for the three rutile crystals TiO_2 , SnO_2 and MgF_2 for the range of indentation testing loads of 10g to 90g. Note the decrease in microhardness with increasing test load

Fig. 2 clearly illustrates the presence of an ISE for these crystals. The ISE is a common phenomenon in all materials [15]. However, in order to achieve a quantitative measure to compare these three ISE values requires representation of the results from a different perspective. As reviewed by Gross and Tomozawa [16], physicists were the first to suggest a power law series to describe hardness data in the ISE regime. This is not unexpected as physicists often use a series approach to describe non-linear results. The power law series that was initially applied to data similar to that in Fig. 2 is:

$$P = a_0 + a_1 d + a_2 d^2 + \text{-------}, \quad (3)$$

Where P is the indentation test load, d is the characteristic impression dimension and the $a_i$are the coefficients. When ISE data are analyzed according to this formula, the first term

of the series, a_0, is observed to be zero and the a_i coefficients above i = 2 are found to be statistically insignificant. This reduces the equation to the two terms, a_1d and a_2d^2 as:

$$P = a_1 d + a_2 d^2. \quad (4)$$

This second order relationship has been derived by two other approaches, one an energy balance and the other a force balance [11]. These independent approaches confirm that the ISE may be described by the above second order equation. Those derivations attribute the a_1 term to surface effects and the a_2 term to volume deformation effects on the observed microhardnesses. Li and Bradt [11] have shown that the a_2 term is related to the load independent microhardness, written as H_{LIH}. By differentiating Equation (4) the load independent hardness, H_{LIH}, is found by setting the slopes of the curves in Fig. 2 equal to zero. The H_{LIH} is only observed or reached for high indentation testing loads as evident from Fig. 2.Frischat [17] has also separated the ISE into a load dependent and a load independent component, also specifying a value for the load independent hardness, H_{LIH}. Although Frischat addressed oxide and chalcogenide glasses, it is evident that the basic concepts are fundamental to indentation hardness and apply to single crystals as well as to glasses.

For the presentation of ISE data and determining of the polynomial coefficients, the experimental data is conveniently represented in a linearized form of Equation (4) as:

$$P/d = a_1 + a_2 d. \quad (5)$$

This equation produces a straight line when presented as (P/d) versus (d) plots for crystals and glasses alike. The ISE data of Fig. 2 is replotted in the form of Equation (5) in Fig. 3. It is evident that the data for all three of these rutile crystal structures can be represented by this linearized expression. The experimental results produce three separate and distinct straight lines with different slopes (a_2 values) and different intercepts (a_1 values). The R^2 values for the lines all exceed 0.99. The 95% confidence intervals for the two regression coefficients of the three crystals, a_1 and a_2 are ~0.01, or less. The regression coefficients for the a_1 and a_2 values for these three rutile crystal structures are listed in Table 3, along with the calculated H_{LIH} values for the crystals.

The H_{LIH} value is the load independent microhardness as determined for the point where the microhardness versus indentation test load slope is equal to zero. Although the results in Fig. 2 do not actually achieve a zero slope over the limited range of test loads which were measured, it appears evident that a zero-slope value would eventually be reached for indentation test loads higher than those in Fig. 2. In Fig. 2 it is evident that a load independent microhardness region exists for higher testing loads, although it is possible that severe indentation cracking may occur before that hardness is reached.

In Table 3 the microhardness values that are reported in the form of the H_{LIH} reflect the order of the measured microhardnesses in the ISE region and previously presented in Figs. 1 and 2. The slopes of the three regression lines and the load independent hardness values, the H_{LIH} are in the order expected from those hardness results. The TiO_2 is the hardest and the MgF_2 is the softest, while the SnO_2 is intermediate in hardness, only slightly softer than the TiO_2. The H_{LIH} values determined via the regression results of Fig. 3 are lower than the measured values reported in Figs. 1 and 2, but this is to be expected for the H_{LIH} is for the zero slope of the hardness vs. indentation test load, while the data in those figures is at lower test load that are still experiencing an ISE. The order of the crystals is as expected for

the softer MgF_2 is a weakened form of the TiO_2 and SnO_2 rutile structures. This is further evident in Fig. 3 for TiO_2 has the steepest slope, a_2 value and the slopes of the straight lines on this plot are related to the load independent hardnesses, the H_{LIH} values.

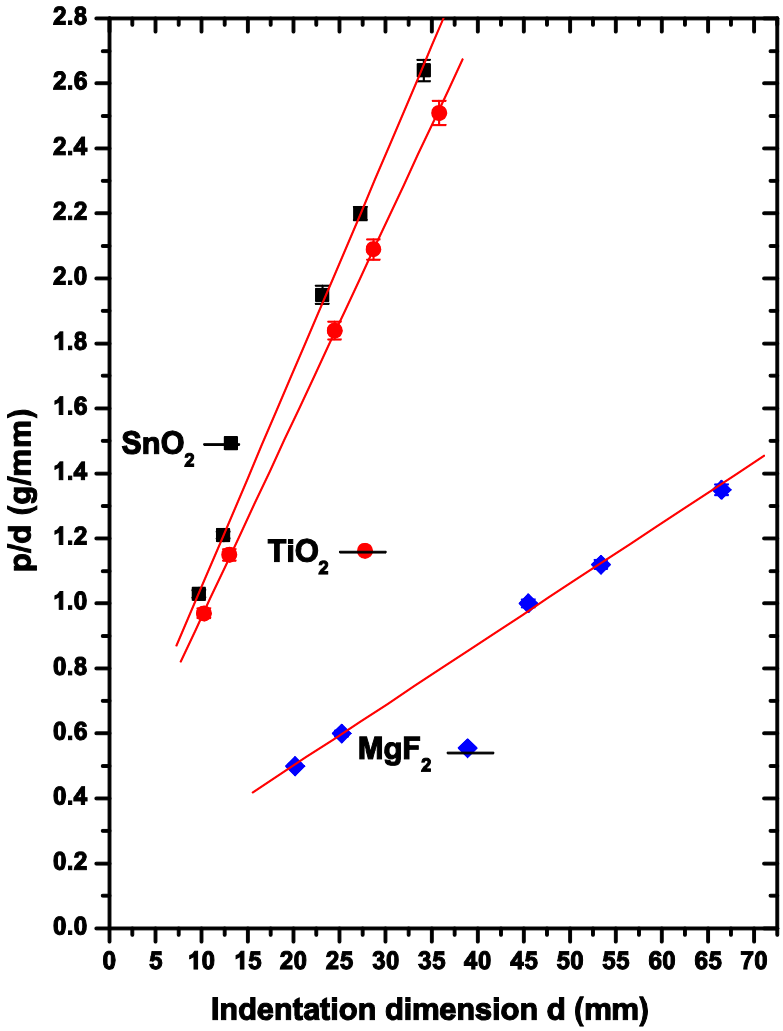

Fig. 3. The ISE for the three rutile crystals, TiO_2, SnO_2 and MgF_2 presented in the linearized form of the second order equation. All are straight lines, but with different slopes, a_2, and also different intercepts, a_1

Table 3. Comparison of the regression lines and microhardnesses of the crystals

Crystal	a_1 (g/μm)	a_2 (g/μm^2)	H_{LIH}(kgf/mm^2)
MgF_2	0.129	0.019	265
SnO_2	0.354	0.061	862
TiO_2	0.387	0.067	947

The a_1 coefficient, the intercept in the linearized plots of Fig. 3, is also a critical parameter for specification of the microhardness for it directly relates to the indentation size effect, the ISE. This can be visualized from the classical power law relationship of Meyer's Law [10] expressing the impression size to the test load as:

$$P = Ad^n. \tag{6}$$

In the absence of any ISE, the n = 2. For n = 2, P is proportional to d^2, a condition which practically never occurs. It would be equivalent to Equation (5), but with the a_1 term equal to zero. There would be no indentation size effect, ISE. It naturally follows that when the Meyer's Law exponent is not equal to two, but lies between one and two, then there must exist an a_1 term in Equation 5 and also an ISE of the indentation test load on the measured indentation hardness. When an ISE is present, the Meyer's Law n-value is less than two, indicative of a non-zero value for the a_1 term in Equations 4 and 5. It follows that one can interpret the magnitude of the ISE as the magnitude of the a_1 coefficient of the power law series. The larger the coefficient a_1, the more prominent is the ISE for the particular material that is being measured. Gross and Tomozawa [16] arrive at the same conclusion for glass, albeit from a slightly different perspective.

Therefore, a larger ISE is present for those materials with larger a_1 values in plots such as that in Fig. 3. This interpretation is in complete agreement with the early results of Atkinson and Shi [18] and Li, et al. [19] for the ISE of dry and lubricated metals and more recently those of Stevenson, et al. [20] for unlubricated and lubricated single crystal hematite. These researchers have shown a decrease in the ISE and also a corresponding decrease in the a_1 value when the specimen surface is lubricated prior to indentation hardness testing. However, in none of the above studies did the lubrication of the test surface change the a_2 values or the H_{LIH} of the microhardness measurements. It only reduces the a_1 value of the second order expression and reduces the amount of the ISE microhardness increase at the lower indentation testing loads.

The magnitudes of the a_1 regression coefficients that are summarized in Table 3 indicate that the ISE is least prominent for the MgF_2 of these three rutile structures for its a_1 value is about one third of that of the rutile, TiO_2 and the cassiterite, SnO_2. Since none of these three crystal specimens were lubricated, but rather indented in their as-polished state, there must be an intrinsic reason for the a_1 value and therefore the ISE of the MgF_2 being less than for the two oxide crystals. Although the details are not understood at the present, following the effects of the lubrication studies above, one explanation may be that the friction between the diamond indenter facets and the MgF_2 crystal surfaces is less than that for either the TiO_2 or the SnO_2.

4. CONCLUSION

The Knoop microhardnesses of single crystal MgF_2 were measured on the (001) basal plane. MgF_2 is a weakened structural analog of TiO_2 and was compared with bothrutile, TiO_2 and also cassiterite, SnO_2 in this paper. The three have the rutile crystal structure. The microhardness anisotropies for each of these three crystals have the same crystal orientations for their maximum and minima of the hardness profiles on their (001) basal planes. This indicates that the three have the same primary slip systems, the {110} <001>. The degree of anisotropy of the three hardness profiles is the greatest for the fluoride, MgF_2. However, the relative hardnesses of the two oxides are substantially greater than for the

MgF_2 as is suggested by the magnitude of the single crystal elastic stiffnesses and consideration of their ionic bondings.

An ISE on the microhardness was observed for MgF_2. It followed the expected increase in the measured Knoop microhardness in the (001) [100] for decreasing indentation testing load. It is the same form as for the two oxides, even though the absolute hardnesses of the crystals are significantly different. The ISE was analyzed by the second order polynomial approach. This form of analysis also confirmed the hardness differences of the crystals and presented a quantitative estimate of the madnitude of the ISE. The ISE is much greater for the two oxides, TiO_2 and SnO_2 which also have the rutile structure than it is for the fluoride, MgF_2 which has the same crystal structure. The reason for this difference is not known with certainty at this time.

ACKNOWLEDGEMENTS

The authors are grateful to Corning Tropel for supplying the MgF_2 single crystals that were measured in this study and to R. Morris for assistance with the diamond polishing of the specimens. The financial support of L. Zhang for summer research by NSF# 0907673 for which V. Acoff and M. Weaver were co-PI's is appreciated.

COMPETING INTERESTS

Authors have declared that no competing interests exist.

REFERENCES

1. Szymanski A, Szymanski JM. Hardness Estimation of Minerals, Rocks and Ceramic Materials. Mat. Sc. Mono. Elsevier Sc. Pub. Inc., NYC, NY. 1989;49.
2. McColml J. Ceramic Hardness. Plenum Pub. Co., NYC, NY; 1990.
3. Swain MV, Bradt RC. Nano- and Micro-Hardness of Single Crystal Yttrium Aluminum Garnet (YAG) on the (111) Plane. In Proc. of the Snowbird Intern. Symp. On Plastic Def. of Ceramics. Plenum Publ. Co., NYC, NY. 1995;195-206.
4. Reister L, Blau PJ, Lara-Curcio E, Breder K. Nanoindentation with a Knoop Indenter. Thin Solid Films. 2000;377-78:635-639.
5. Li H, Bradt RC. Knoop Hardness Anisotropy of Single-Crystal Rutile. J. Amer. Cer. Soc. 1990;73(5):1360-1364.
6. Li H, Bradt RC. Knoop Hardness Anisotropy of Single-Crystal Cassiterite. J. Amer. Cer. Soc. 1991;74(5):1053-1060.
7. Li H, Bradt RC. The microhardness indentation load/size effect in rutile and cassiterite single crystals. J. Mat. Sc. 1993;28:917-926.
8. Corning Tropel. Fairport, NY, USA. 2008;14450-1328.
9. Buehler, Ltd., Lake Bluff, IL, USA. Buehler Micromet 2004 Testing Manual: 2004.
10. The Science of Hardness Testing, edit by J. Westbrook and H. Conrad, ASM, Metals Park, OH; 1973.
11. Li H, Bradt RC. The Knoop Hardness Anisotropy of Single Crystal LaB_6. Mat. Sc. and Eng. A. 1991;142(1):51-61.
12. Hirthe WM, Adsit NR, Brittain JO. Dislocations and Plastic Deformation in Titanium Dioxide Single Crystals. The Direct Observatioin of Imperfections in Crystals, edited by J.B. Newkirk, Interscience Publishers, NY, NY. 1962;135-162.

13. Chung DH, Buessem WR. The Elastic Anisotropy of Crystals. Anisotropy of Single Crystal Refractory Compounds, edited by F.W. Vahldiek and S.A. Merson, Plenum Press, NY, NY. 1968;2:217-245.
14. Simmons G, Wang H. Single Crystal Elastic Constants and Calculated Aggregate Properties. The MIT Press; 1971.
15. Kleiner D, Durst K, Rester M, Minor AM. Revealing Deformation Mechanisms with Nanoindentation. Journal of Metals. 2009;61(3):14-23.
16. Gross TM, Tomozawa M. Fictive temperature-independent density and minimum indentation size effect in a calcium aluminosilicate glass. JAP. 2008;104(6):063529-063529-10.
17. Frischat GH. Load-Independent Microhardness of Glasses. Strength of Inorganic Glasses, edit by C.R. Kurkjian. Plenum Press, New York, NY. 1985;135-145.
18. Shi H, Atkinson M. A friction effect in low load hardness testing of copper and aluminum. J. Mat. Sc. 1990;25:2111-2114.
19. Li H, Ghosh A, Han YH, Bradt RC. The friction component of the indentation size effect in low load microhardness testing. J. Mat. Res. 1993;8(5):1028–1032.
20. Stevenson ME, Kaji M, Bradt RC. Microhardness Anisotropy and the Indentation Size Effect on the Basal Plane of Hematite. J. Eur. Cer. Soc. 2002;22:1137-1148.

Peer-review history:
The peer review history for this paper can be accessed here:
http://www.sciencedomain.org/review-history.php?iid=283&id=4&aid=2206